Journal of Materials Chemistry B

ROYAL SOCIETY OF CHEMISTRY

PAPER

View Article Online
View Journal | View Issue



Check for updates

Cite this: J. Mater. Chem. B, 2025, 13, 5358

# Utilizing an aqueous-liquid crystal interface to investigate membrane protein interactions and mutation effects of a pore-forming toxin†

Tarang Gupta,‡[a] Kusum Lata,‡[b] Kausik Chattopadhyay*[b] and Santanu Kumar Pal *[a]

Received 21st September 2024,
Accepted 19th March 2025

DOI: 10.1039/d4tb02117g

rsc.li/materials-b

Listeriolysin O (LLO) is a crucial cholesterol-dependent cytolysin (CDC) secreted by *Listeria monocytogenes*. LLO lyses the phagosomal membrane *via* pore-formation, resulting in pathogenesis. CDCs' ability to recognize and bind to membrane cholesterol is a hallmark in the pathogenesis of these pore-forming toxins, distinguishing them from other toxins. Conservation of the cholesterol-recognition motif (CRM) has been discovered to be one of the prerequisites for the membrane binding of some CDCs, but the role of the CRM for LLO binding and pore-formation is still unclear. Therefore, we investigated LLO-mediated lipid remodelling at a nanomolar concentration using the interfacial properties of a biomimetic liquid crystal (LC)–aqueous interface. The examination addresses the significance of the CRM in protein structure and membrane reorganizations for the cholesterol-mediated binding of LLO. We report that the CRM assists in the binding of LLO in a unique amphipathic environment, especially at low cholesterol levels. However, eliminating or substituting the CRM from LLO significantly alters the threshold cholesterol level required for its activity. This study also reveals the effect of cholesterol-dependent membrane dynamics in the association and activity of LLO. Our findings suggest a novel paradigm that opens up an array of possibilities for discovering sequential mutations and delineating the molecular mechanisms of CDCs in nanomolar concentration regimes.

## Introduction

Cholesterol-dependent cytolysins (CDCs) represent a widely disseminated family of pore-forming toxins (PFTs) employed mostly by Gram-positive bacteria, including *Bacillus*, *Streptococcus*, *Clostridium*, and *Listeria*, which are human pathogens.[1] The CDCs assist in pathogenesis mainly by disrupting the host epithelial barrier through pore-formation and modulating the host immune system.[2] All CDCs share a four-domain tertiary structure and exhibit a cholesterol-dependent pore-forming and cytotoxic activity.[3] The presence of cholesterol in the target membrane is a prerequisite for the activity of CDCs. Interestingly, studies have demonstrated that cholesterol is not necessarily required for the binding, but for the further steps of pore-formation. The primary interaction of CDCs with cholesterol has been mapped to a threonine and leucine (Thr-Leu) pair in the loop (L1) of domain 4.[4] These investigations have characterized the cholesterol-recognition motif (CRM) for a few CDCs, including perfringolysin O (PFO), pneumolysin (PLY), and intermedilysin (ILY). In the present study, we have explored the cholesterol-dependent interaction of a prominent member of the family, listeriolysin O (LLO). LLO is the major virulence factor secreted by *L. monocytogenes*, a food-borne intracellular pathogen.[5] One notable distinction between LLO and other CDCs is its proactive role in aiding pathogens to remain within the host cells.[6] The high immunogenicity of LLO gives it exceptional medicinal importance, highlighting the significance of its research. It is understood that it binds to the cholesterol-containing phagosomal membrane, which aids the pathogen's egress from the phagosome to the cytosol through transmembrane β-barrel pores of size up to 50 nm. It has been previously reported that a CRM, conserved in all CDCs, facilitates the binding of CDCs to cholesterol-containing lipid membranes,[4] but the precise mechanistic details of cholesterol-mediated pore-formation by LLO and other CDCs remain to be fully elucidated. We propose that some concurrent alterations in membrane dynamics, such as lipid mixing, lipid flipping, or lipid domain

[a] Department of Chemical Sciences, Indian Institute of Science Education and Research Mohali, Knowledge City, Sector-81, SAS Nagar, Mohali 140306, India. E-mail: skpal@iisermohali.ac.in, santanupal.20@gmail.com
[b] Department of Biological Sciences, Indian Institute of Science Education and Research Mohali, Knowledge City, Sector-81, SAS Nagar, Mohali 140306, India. E-mail: kausik@iisermohali.ac.in

† Electronic supplementary information (ESI) available: Materials and methods, and different POM images, control experiments, and dynamic views. See DOI: https://doi.org/10.1039/d4tb02117g

‡ These authors have contributed equally.

reorganizations, may be beneficial in regulating this pore-formation mechanism and need to be acknowledged. In a recent study, it was shown that a CRM-altered variant of LLO can bind to cholesterol-rich membranes under specific conditions. While this mutant variant does not bind effectively to membranes with absent or minimal cholesterol, its binding becomes comparable to that of wild-type LLO when an optimal cholesterol level is present. Such binding behavior of the CRM-altered LLO variant has been shown to be facilitated by lipid phase heterogeneity due to optimal cholesterol levels. Overall, this study has revealed the complex interplay between cholesterol, the CRM motif, and the lipid environment during LLO-mediated membrane disruption.[7] This intricate relationship calls for more advanced experimental approaches to unravel the molecular mechanisms of CDCs within the context of the physicochemical properties of lipid membranes.

Past studies have identified liquid crystals (LCs) as stimulus-responsive materials due to the combination of fluidity and orientational order that enables dynamic self-organization.[8] The interfaces generated between thermotropic LCs and aqueous phases are especially interesting for reporting interactions involving biological organisms for three major reasons: (i) biomolecular binding events can be observed without any fluorescent labelling, (ii) the interfaces are dynamic, and species can be reorganized laterally in ways that resemble biomolecular interactions at biological membranes, and (iii) the experimental setup is straightforward, and may be applicable for the creation of diagnostics for usage in resource-constrained settings. Hence, LC-based transduction has been widely exploited to amplify the presence of a range of chemical and biological species (lipids, proteins, DNA, and mammalian and bacterial cells) at interfaces into optical signals.[9]

Inspired by this, our previous research sought to establish that LC–aqueous interfaces have the potential to replicate the cholesterol-mediated membrane interactions of *Vibrio cholerae* cytolysin (VCC) at physiological concentrations.[10] Advancing our study, we ask whether a biomimetic LC–aqueous interface could capture the LLO-mediated modulations to the unique amphipathic environment. In addition, the present study focuses on understanding the LLO–cholesterol interaction mediated by the CRM, which aids membrane binding and activity. The CRM motif in LLO was substituted with a pair of glycines to generate the $LLO^{T515G\text{-}L516G}$ form of LLO to investigate the cholesterol-dependent membrane interactions and modulations by LLO.

We report that the mutation of the CRM region significantly affected the ability of LLO to physically interact with cholesterol. However, the binding ability was reduced only when there was a low amount of cholesterol in the membranes, suggesting an effect of cholesterol and membrane dynamics on the activity of LLO. Also, cholesterol can be a key player in modulating the phase heterogeneity, packing, and hydrophobicity of lipids in membranes.[11] This study scrutinized the potential of the LC–aqueous interface to recognize the substitution of two amino acids based solely on LC optical responses under physiological environments. As a result, the LC-based method might be endorsed as the easiest assay to examine the structural basis and cholesterol-dependent pathogenicity of proteins produced by bacteria. Overall, our research aims to comprehend the lipid–protein interactions occurring at the aqueous interface of LC at the nanoscale, which conventional measurement tools cannot access. However, there is still scope for further research on the interaction between membrane dynamics and LLO activity.

## Results and discussion

For *in vitro* insights into LLO actions towards the membrane, we first mimic a unique amphipathic membrane environment by self-assembling 1-palmitoyl-2-oleoyl-*sn*-glycero-3-phosphocholine (PC) at a thermotropic liquid crystal (LC) 5CB (4′-pentyl-4-biphenylcarbonitrile)–aqueous interface. For our initial set of experiments, we began by encapsulating 5CB using a TEM-gold grid supported on a glass substrate coated with dimethyloctadecyl[3-(trimethoxysilyl)propyl]ammonium chloride (DMOAP) under phosphate-buffered saline (PBS; pH = 7.2). We observed that the thin films of 5CB exhibited a bright optical appearance under a polarizing optical microscope (POM) when immersed in PBS, consistent with the prior reports.[9] Subsequently, we sought to investigate the orientational behaviour of 5CB in various concentrations of PC. We observed that on the introduction of 0.01 mg $ml^{-1}$ of PC, the appearance of 5CB became partially dark with scattered bright domains, persisting for approximately 30 min (Fig. 1a, first row). However, upon increasing the PC concentration to 0.03 mg $ml^{-1}$, we observed a completely dark appearance under POM, as depicted in Fig. 1a. As expected, on further increase in the PC concentration to 0.05 mg $ml^{-1}$, the dark optical view remained intact.

Our second goal was to gain insights into the interactions between LLO and the distinctive membrane environments formed by lipid mixtures of cholesterol and PC. For this, we conducted a second set of experiments to analyze the ordering pattern of 5CB in the presence of PC vesicles containing 15 and 30-wt% cholesterol. The rationale behind this objective was rooted in the observation that cholesterol plays a vital role in enabling LLO to form pores in target membranes.[3] We first experimented with 0.01 and 0.03 mg $ml^{-1}$ lipid mixtures (15 or 30 wt% cholesterol into PC vesicles).

Interestingly, we observed that the added lipid mixture did not result in a completely dark optical appearance of LC within 30 min (Fig. 1a, second and third rows). However, when the concentration of the lipid mixture was increased to 0.05 mg $ml^{-1}$, a completely dark optical appearance of the LC was observed. The variation in the ordering pattern of 5CB depending on the % of cholesterol in PC is consistent with our previous findings that suggest that the rigidity imposed by cholesterol and the reduction in PC density within the vesicles are likely contributing factors to this phenomenon.[10]

Next, we sought to observe the role of CRM in LLO for its activity towards lipid membranes having 15 and 30 wt% cholesterol. To monitor this, we designed an LLO mutant by substituting two amino residues, *i.e.*, Thr-Leu in LLO, with a pair of glycines (Gly-Gly). The mutant is designated as $LLO^{T515G\text{-}L516G}$. Before analyzing their behaviour at the LC–aqueous interface in the

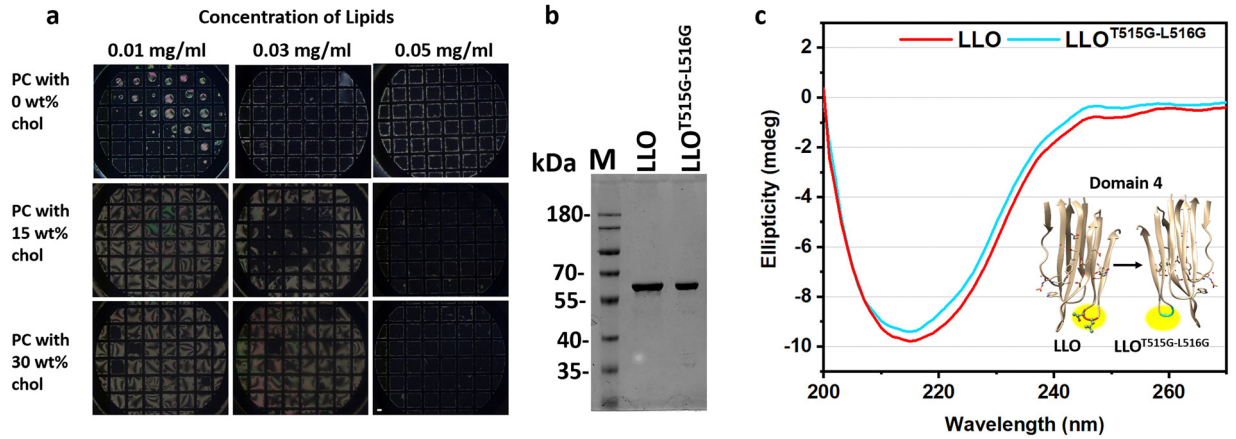


Fig. 1 (a) Polarized optical photomicrographs of the LC–aqueous interface depicting the LC response after 30 min of incubation with 0, 15, and 30 wt% cholesterol in PC. The optical views display a uniformly dark appearance of LC at 0.03 mg ml$^{-1}$ PC and 0.05 mg ml$^{-1}$ lipid mixture (PC having 15 or 30 wt% cholesterol). Scale bar = 100 μm. The data are consistent with an earlier study[10] and have been reperformed for further investigation. (b) The SDS-PAGE/Coomassie staining profile displaying the purified LLO and its mutant LLO$^{T515G-L516G}$. Lane M depicts the molecular weight markers. (c) CD spectra illustrating the β-sheet rich nature of both LLO and its mutant LLO$^{T515G-L516G}$. The structure of domain 4 of LLO and LLO$^{T515G-L516G}$ is shown in the inset of (c) (PDB ID 4CDB, image generated in Chimera).

presence of lipid mixtures, we first assessed the quality of protein purification using SDS-PAGE, followed by Coomassie staining. This confirmed the purity of LLO and its mutant, LLO$^{T515G-L516G}$ (Fig. 1b). We then investigated the structures of both proteins by recording far-UV circular dichroism (CD) spectra. The spectra shown in Fig. 1c demonstrate the β-sheet-rich nature of LLO, which remains intact after the glycine substitutions. Additionally, almost identical ellipticities of both proteins showed the similar structural disposition of LLO and its mutant.

Based on the above information, we sought to monitor the activity of LLO and its mutant LLO$^{T515G-L516G}$ at the LC–aqueous interface laden with lipid mixtures. This experiment aimed to ascertain whether the lipid-enriched aqueous interfaces of LCs could indicate the binding of LLO and its mutant LLO$^{T515G-L516G}$ at physiologically relevant concentrations (*i.e.*, within the nM range). Numerous studies have shown that when proteins are introduced into the lipid layer in contact with LC-aqueous films, the LCs are reorientated. This change in the optical response of the LCs upon lipid–protein binding is related to the secondary structure of the protein. Proteins characterized by a predominant β-sheet-rich secondary structure induce dendritic patterns in LCs.[12] Keeping this concept in mind, we observed the optical behaviour of LC at the LC–aqueous interface adorned with lipid mixtures (15 and 30 wt% cholesterol in PC) upon introducing 100 nM LLO and LLO$^{T515G-L516G}$. We made three observations based on the optical images presented in Fig. 2a, captured at 1 and 30 min upon adding 100 nM proteins at those interfaces. First, we observed the emergence of bright optical domains shortly after 1 min of addition of LLO and LLO$^{T515G-L516G}$ to the lipid mixture-decorated interface. Interestingly, this emergence of bright domains was more pronounced in the lipid mixture of 30 wt% cholesterol in PC than in the mixture with 15 wt% cholesterol in PC. Second, we observed the transformation of initially uniformly dark areas into completely bright areas after 30 min of addition of proteins to the 30 wt% cholesterol/PC lipid mixture laden at the LC–aqueous interface. This change indicated a significant alteration in the optical properties of the LC over time. The third observation revealed that the presence of dendritic domains was more pronounced when LLO was added to the lipid mixture containing 15 wt% cholesterol in PC, as compared to its mutant variant LLO$^{T515G-L516G}$, at the LC–aqueous interface. This suggests that LLO substantially influences the formation and growth of dendritic structures in this particular lipid composition. To further provide insights into the variations in the extent of the formation of optical domains, we conducted quantitative measurements. We calculated the mean grayscale intensities of the LC–aqueous interface laden with different lipid mixtures (PC/30 and 15% cholesterol) in the presence of LLO and LLO$^{T515G-L516G}$ (Fig. 2b). The box graphs displayed a significant difference in the mean grayscale intensities of 15 wt% cholesterol in PC (Fig. 2d) than 30% in the PC (Fig. 2c) laden LC–aqueous interface in the presence of LLO and LLO$^{T515G-L516G}$. This observation indicates the prominent binding of LLO with 15 wt% cholesterol in PC compared to LLO$^{T515G-L516G}$. In order to verify that the emerged dendritic domains are the result of LLO and LLO$^{T515G-L516G}$–lipid interactions at the aqueous interfaces of LC, we performed two additional control experiments. First, we incubated 200 nM LLO and LLO$^{T515G-L516G}$ at the LC–aqueous interface without any lipid. Notably, no change in the optical appearance was observed over a prolonged time, and it did not form any branched domains (Fig. S1, ESI†). Second, we incubated 100 nM of LLO at the lipid mixture (15 wt% cholesterol in PC)-laden LC–aqueous interface. We observed the formation of bright dendritic domains under POM, which were also visible after the removal of analyzers, indicating modulations in the lipid density due to protein interactions at those interfaces (Fig. S2a–d, ESI†). These data sets confirmed that the evolution of brush-like patterns results from the transduction of lipid–protein interactions to the LC.

At this stage, we aimed to analyze the elongated branched domains arising from LLO interactions with lipid mixtures

 

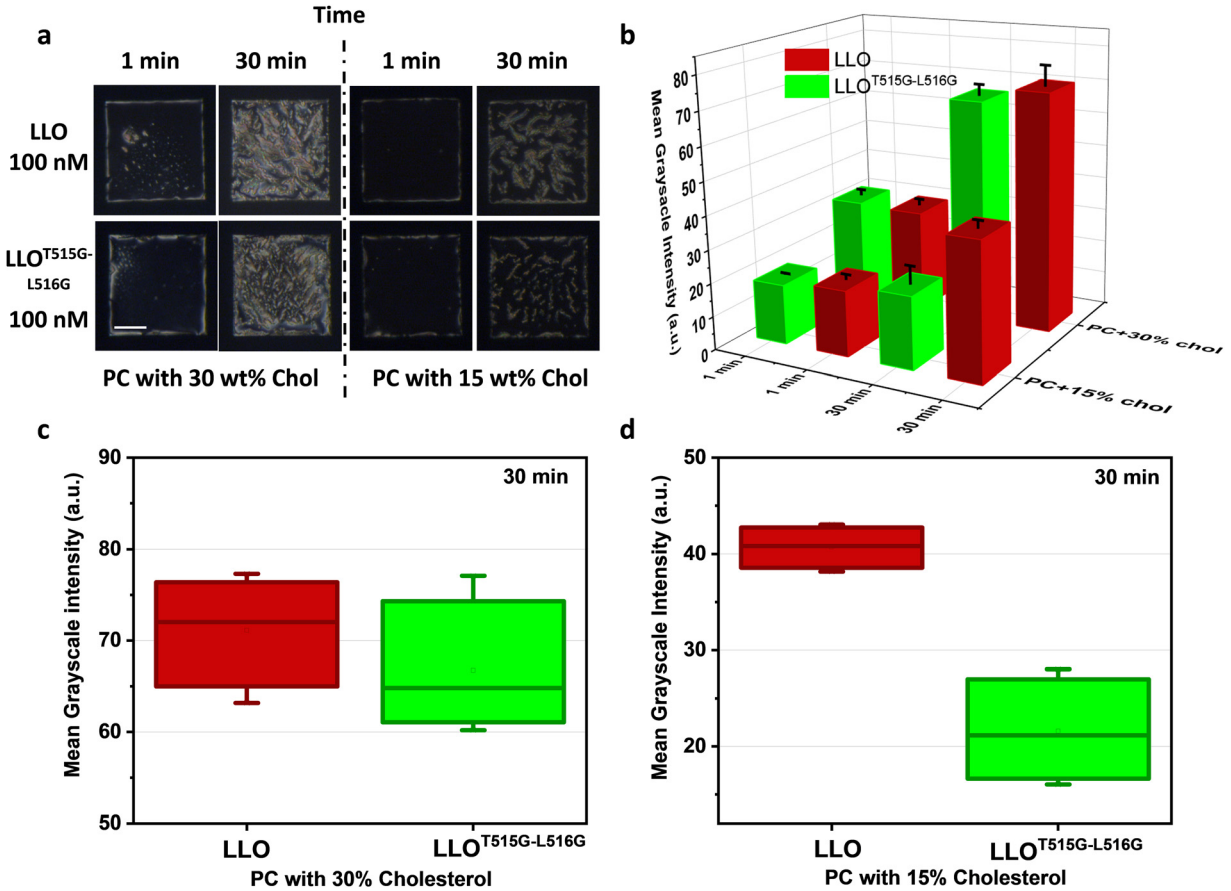


Fig. 2 (a) Polarized photomicrographs depicting the differential densities of the optical domains after 1 and 30 min incubation of 100 nM LLO and its mutant LLO$^{T515G-L516G}$ with 30 and 15 wt% cholesterol in the PC-laden LC–aqueous interface. Scale bar = 100 μm. (b) Bar graph illustrating the average mean grayscale intensities (four grid squares) at 1 and 30 min incubation of LLO and LLO$^{T515G-L516G}$ at the designed interfaces. (c) and (d) Box plot illustrating the distribution of mean grayscale intensities for LLO and its mutant after 30 min of incubation with PC containing 30 wt% and 15 wt% cholesterol, respectively, present at the LC–aqueous interface. (c) No significant differences ($p$ = 0.4 > 0.05; Anova) were observed in LLO and LLO$^{T515G-L516G}$ interactions with PC/30 wt% cholesterol after 30 min of incubation. (d) A significant difference ($p = 5 \times 10^{-4} < 0.05$; Anova) was observed in LLO and LLO$^{T515G-L516G}$ interactions with PC/15 wt% cholesterol after 30 min of incubation.

present at the LC–aqueous interface. To achieve this, we performed an atomic force microscopy experiment (AFM). The imaging was conducted subsequent to a 30 min incubation of LLO at the interfaces decorated with mixed lipid (PC/30% cholesterol)-LC, followed by drying the extracted aqueous layer from those interfaces. The AFM images unveiled the existence of arc- or slit-shaped assemblies, as well as filamentous structures, measuring approximately 3 nm in height at the interface (Fig. S3a and b, ESI†). Notably, these structures were absent in samples extracted from the LC-LLO devoid of any lipid (Fig. S3c, ESI†) and LC-lipid mixture devoid of LLO (Fig. S3d, ESI†). This observation underscores the role of the lipid mixture and LLO interactions at the interface in forming these assemblies. We postulate that these structures represent lipid mixture-guided LLO oligomeric assemblies at the interface. To validate our hypothesis, we employed a pull-down based oligomerization assay followed by SDS-AGE (agarose gel electrophoresis)/Coomassie staining to visualize the formation of LLO oligomers on the mixed lipid (PC/30% cholesterol)-LC-decorated interfaces. Our results demonstrate that LLO does not form oligomers in the presence of LC alone. Additionally, lipid-laden LC alone could not induce the formation of the LLO oligomers. However, LLO oligomers were observed only when LC droplets were loaded with lipids, similar to those formed with liposomes (Fig. S3e, ESI†). The observation of oligomeric assembly formation is concordant with an earlier study.[13] These findings confirm that LLO undergoes oligomerization through dynamic fusion events at the interface. This process is facilitated by chemoresponsive LC,[14] thereby inducing the emergence of distinctive branched patterns at the interfaces.

Our next goal was to gain insights into the progression of events over time and to understand the initial dynamics of interactions of proteins with different cholesterol concentrations. In this regard, we investigated the time-lapsed behaviour of both LLO and its mutant variant LLO$^{T515G-L516G}$ in the presence of lipid mixtures containing 30 wt% and 15 wt% cholesterol in PC at the LC–aqueous interface. First, we monitored the LC response laden with PC having 30 wt% cholesterol when placed in contact with LLO and LLO$^{T515G-L516G}$. Fig. S4 (ESI†) reveals an almost similar kinetics of LLO and LLO$^{T515G-L516G}$ activity with 30 wt% cholesterol in PC at higher (100 nM) as well as at lower concentrations

(10 nM). This outcome suggests that the ability of LLO to bind to a mixture of 30 wt% cholesterol and PC lipids is uncurbed by the existence of the CRM in the protein.

Then, we analysed the activity of proteins with a lipid mixture of 15 wt% cholesterol in PC. The time-lapsed images of 100 and 50 nM LLO and LLO$^{T515G-L516G}$ displayed considerable differences in the activity of the proteins. The emergence of dendritic domains was found to be much faster for LLO compared to LLO$^{T515G-L516G}$ (Fig. S5a, ESI†). Furthermore, the quantification of interactions through the mean grayscale intensity difference supports our preposition of pronounced binding of LLO with PC having 15 wt% cholesterol compared to its mutant LLO$^{T515G-L516G}$ (Fig. S5b–d, ESI†). This observation also holds at lower concentrations of proteins, *i.e.*, at 25 nM (Fig. S6, ESI†). However, after further decreasing the concentration to 10 nM, no changes in LC ordering were observed, suggesting that the sensitivity of the designed system was up to 25 nM (Fig. S6, ESI†). To validate our observations, we performed a pull-down-based binding assay to assess the interaction between LLO and its mutant, LLO$^{T515G-L516G}$, with lipid mixture liposomes (Fig. S7, ESI†). The percentage of liposome-bound LLO and LLO$^{T515G-L516G}$ was quantified by analyzing the band intensities in the gel profile using ImageJ software, with the values indicated below the gel. The nearly identical band intensities for both LLO and LLO$^{T515G-L516G}$ demonstrated binding to PC vesicles containing 30 wt% cholesterol, as indicated by the presence of protein in the liposome-bound pellet fraction. In contrast, a significant difference in band intensities was observed when using PC vesicles with 15% cholesterol. LLO showed binding to the liposomes, as evidenced by the protein in the liposome-bound pellet fraction, while LLO$^{T515G-L516G}$ predominantly remained in the unbound supernatant fraction, suggesting a lack of binding under these conditions. These results further support our initial observations. Subsequently, we sought to determine the relationship between the spatial patterns of LC and the lateral distribution of lipids and proteins at those interfaces. To comprehend this, we performed confocal fluorescence microscopy to enquire about the localization of lipids and proteins at the aqueous–LC interface. The 15 wt% cholesterol in PC doped with 2.5% fluorescently labelled PC (Cy5 PC) was self-assembled at the LC–aqueous interface and incubated with Alexa 488-labelled LLO and LLO$^{T515G-L516G}$ for up to 30 min. Like our above observation, we noticed the growth of dendritic patterns visible under the bright field of the confocal microscope (Fig. 3a and d). In addition, the fluorescence images illustrated that green-fluorescent protein accumulated in the form of dendritic patterns (Fig. 3b and e) and surrounding them is red fluorescence (Fig. 3c and f). This suggests the lateral distribution of protein- and lipid-rich regions, where dendritic patterns are protein-rich. Thus, our data indicate the phase segregations of lipids and proteins at the designed interfaces. Overall, the key findings from our observations are: (i) β-sheet rich nature of LLO and LLO$^{T515G-L516G}$, as observed from the emerging dendritic patterns[12] for both the proteins at the interface, which is also evident from the CD spectra; (ii) CRM substitution lowers the activity of LLO at lower cholesterol content in the membrane.

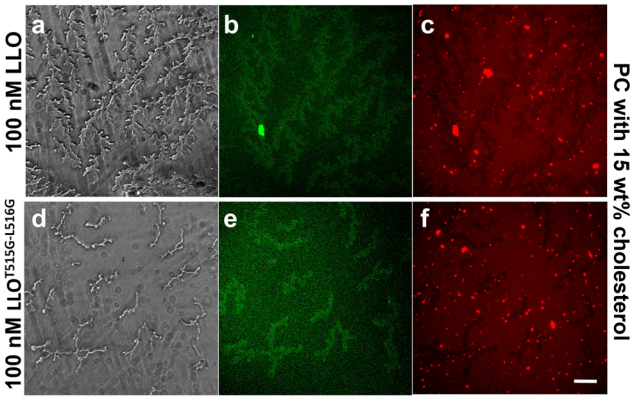


Fig. 3 (a) and (d) Bright-field and (b), (c), (e) and (f) confocal fluorescence images of Alexa-488-labelled LLO and LLO$^{T515G-L516G}$ after 30 min of incubation with 2.5% cy5 labelled PC doped in PC having a 15% cholesterol lipid mixture-decorated LC–aqueous interface. Green fluorescence in (b) and (e), and dark branched domains in (c) and (f) depict protein-rich domains, and surrounding them is a lipid-rich region. Scale bar = 20 μm.

This indicates that the Thr-Leu dipeptide binds cholesterol more strongly than a pair of Gly-Gly amino acids.

Next, we aimed to investigate the factors contributing to the similar and differential responses of LLO and LLO$^{T515G-L516G}$ proteins under high and low cholesterol content conditions. The experiment aimed to address two primary goals. First, we sought to investigate whether the observed results of the superior binding of LLO with cholesterol compared to its mutant were solely due to unique interactions between the cholesterol and proteins. Second, we aimed to find whether these results were a consequence of cholesterol-induced impacts on the lipid assemblies at the interface. To address these questions, we conducted a control experiment in which 100 nM proteins were added to the LC laden with a lipid mixture containing 15 wt% ergosterol in PC. We then observed the system for a duration of up to 30 min following the addition of 100 nM LLO and LLO$^{T515G-L516G}$ proteins. This control experiment allowed us to assess the role of ergosterol in influencing the observed results and to gain insights into the specific effects of cholesterol on the lipid assemblies at the interface. The optical images in Fig. S8a (ESI†) illustrate a similar response of both proteins at the lipid-mixture (PC/15 wt% ergosterol)-laden LC–aqueous interface. Additionally, this observation is confirmed through measurements of mean grayscale intensities (Fig. S8b, ESI†) and their distributions (Fig. S8c, ESI†). This suggests the involvement of the CRM in the specific recognition of cholesterol. Subsequently, we designed an experiment to investigate the impact of cholesterol-dependent lipid dynamics on the response of LC in the presence of LLO. We experimented using 0.0425 mg ml$^{-1}$ PC alone, a concentration equivalent to that in PC/15 wt% cholesterol mixtures, to examine the dependence of LC orientational response on various factors mentioned above. Remarkably, we observed negligible response of PC-laden LCs in the presence of 100 nM LLO (Fig. S9, ESI†), highlighting the significant impact of cholesterol-mediated lipid dynamics on the interaction between LLO and lipid membranes. Based on our findings, we can make three fundamental statements about the

 

bindings of both proteins. First, at low cholesterol concentrations, LC laden with a lipid mixture exhibit a distinctive response when exposed to LLO and LLO$^{T515G-L516G}$, which differs from their response at higher cholesterol concentrations. Second, substituting the lower amount of cholesterol with ergosterol eliminates the disparity in the activity of both proteins. Third, no PC-laden LC response was noticed in LLO's presence. These observations suggest that LLO can be associated with lipids even without CRM-mediated cholesterol interaction only when cholesterol is abundant. However, CRM-mediated cholesterol interactions are necessary to associate LLO with a nominal amount of cholesterol. This could be explained by the fact that some additional parameters may support the binding of LLO in the absence of the CRM, with lipid membranes having a high cholesterol concentration. It has already been established that a high amount of cholesterol would increase the hydrophobicity, degree of order, and heterogeneity in the membrane, leading to distinct dynamics of the lipid layer.[10] These changes in the lipid environment may intensify non-covalent hydrophobic interactions of proteins with the lipid membranes and their partitioning into distinct lipid phases of the membrane, which can account for the similar responses of LLO with and without the CRM. However, at low concentrations of cholesterol, not much impact is known on lipid dynamics. Therefore, the importance of the CRM for the activity of LLO increases. This proposition is also supported by a control experiment with 15% ergosterol. With a 15% ergosterol PC mixture, the similar response of LC in the presence of proteins indicates the importance and specificity of cholesterol in the binding of LLO with the lipid membranes. A schematic illustration of the binding of LLO and its mutant, LLO$^{T515G-L516G}$, at the lipid mixture (PC with 15% and 30% cholesterol)-laden LC–aqueous interface is presented in Fig. 4. Our study highlights the LC–aqueous interface as a powerful and versatile tool for investigating the interactions of membrane proteins, such as pore-forming toxins (PFTs), with lipid membranes. Specifically, we utilized this interface to examine the effects of mutations on LLO and its membrane interactions. Notably, the membrane-composition-dependent behaviour of LLO was observed, indicating the high sensitivity of the aqueous–LC interface-based approach in detecting subtle changes in protein–lipid interactions.

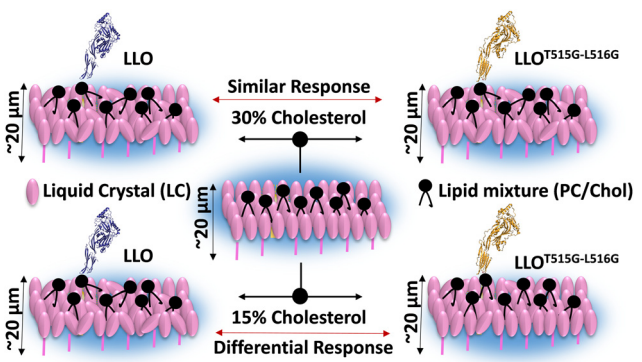


Fig. 4 A schematic illustration to represent the changes induced in the liquid crystal (LC) ordering by the addition of LLO and LLO$^{T515G-L516G}$ at the lipid mixture-laden LC–aqueous interface. The cartoons demonstrate similar responses of LC–aqueous interfaces laden with lipids containing 30% cholesterol in the presence of LLO and LLO$^{T515G-L516G}$, compared to those containing 15% cholesterol. The structural model of LLO was generated with PyMOL (The PyMOL Molecular Graphics System, Version 2.5.2 Schrodinger, LLC.) using the Protein Data Bank (PDB) ID 4CDB.

Building on our previous work with *Vibrio cholerae* cytolysin,[10] we demonstrate that the LC–aqueous interface provides a controlled environment to study the membrane association of PFTs. The complementary use of AFM imaging and pull-down assays further corroborated our findings, confirming the differential binding properties of LLO variants on membranes with varying cholesterol content. These results validate the sensitivity of the LC–aqueous interface in studying PFT interactions and underscore the interdisciplinary nature of this approach, combining advanced biophysical techniques to deepen our understanding of PFT function and membrane dynamics. Overall, our findings indicate the interplay of lipid membrane dynamics and cholesterol dependency in the binding of LLO. The CRM's ability to assist in the binding of LLO in an amphipathic environment, especially at low cholesterol levels, indicates its critical role in the pathogenicity of *L. monocytogenes*. This study provides broader implications for understanding other CDCs and their roles in various infections, shedding light on common mechanisms that might be targeted in drug development.

## Conclusions

In a nutshell, this study demonstrated the sophisticated mechanism of LLO binding towards various membranes through the simplest method of using an LC–aqueous interface as a potent hosting platform. This work displayed the varied membrane-binding abilities of LLO and its mutant LLO$^{T515G-L516G}$ on lipid membranes hosted on LCs, highlighting the crucial function of the CRM in the binding of LLO. The results indicated the remodelling of lipid membranes having 30–15 wt% cholesterol in zwitterionic lipid-PC to dendritic domains. A comparison of evolution rates of dendritic domains revealed the interplay of membrane dynamics and the role of the CRM in the modulation of LLO binding to lipid membranes. At lower cholesterol concentrations, CRM mutations render low activity of LLO, which contrasts with high cholesterol levels. High cholesterol in lipid membranes would support LLO by modulating the lipid nature, thus decreasing the impact of CRM mutation in the LLO. Thus, our study provides valuable insights into the binding and interaction mechanisms of LLO with lipid membranes, particularly at concentrations of 25 nM and above. In contrast to conventional techniques, which often require sophisticated instrumentation, extensive labor, complex labelling protocols, and time-consuming procedures, our approach simplifies characterizing LLO–lipid interactions. By streamlining the methodology, we facilitate investigation, yielding significant insights without the challenges typical of traditional methods. This robust framework enhances our understanding of the underlying mechanisms governing these interactions, making it easier to draw meaningful conclusions and paving the way for

future studies. Altogether, our research embraces the LC–aqueous interface as an augmentative tool to detect differences in protein activity on mutations of just two amino acids. Our study substantially strengthens the understanding of CDCs' binding behaviour, which has significant clinical implications.

## Data availability

The data supporting this article have been included as part of the ESI.†

## Conflicts of interest

There are no conflicts to declare.

## Acknowledgements

S. K. P. acknowledges MOE/STARS/284. T. G. thanks CSIR (09/947/(0223)/2019EMR-1) for the fellowship. K. L. thanks CSIR (09/947/(0111)/2019-EMR-1) for the fellowship. We acknowledge Dr Gregor Anderluh, Kemijski inštitut/National Institute of Chemistry, Slovenia, for providing the Nucleotide construct of LLO in the pPROEX HTb vector. We have used the PyMOL Molecular Graphics System (Version 2.5.2 Schrodinger, LLC.), Protein Data Bank (PDB) ID 4CDB and chem draw software for drawing protein and chemical structures, respectively, in the TOC graphic. This work is a part of the PhD Thesis of one of the co-authors, T. G., at IISER Mohali (PhD Thesis defended: Year 2024).[15]

## Notes and references

1 S. Koster, K. van Pee, M. Hudel, M. Leustik, D. Rhinow, W. Kuhlbrandt, T. Chakraborty and O. Yildiz, *Nat. Commun.*, 2014, **5**, 3690.
2 J. E. Alouf, *Curr. Top. Microbiol. Immunol.*, 2001, **257**, 1–14.
3 R. K. Tweten, *Infect. Immun.*, 2005, **73**, 6199–6209.
4 A. J. Farrand, S. LaChapelle, E. M. Hotze, A. E. Johnson and R. K. Tweten, *Proc. Natl. Acad. Sci. U. S. A.*, 2010, **107**, 4341–4346.
5 K. Lata, M. Singh, S. Chatterjee and K. Chattopadhyay, *J. Membr. Biol.*, 2022, **255**, 161–173.
6 B. N. Nguyen, B. N. Peterson and D. A. Portnoy, *Cell. Microbiol.*, 2019, **21**(3), e12988.
7 K. Lata, G. Anderluh and K. Chattopadhyay, *Biochem. J.*, 2024, **481**(19), 1349–1377.
8 (*a*) V. K. Gupta, J. J. Skaife, T. B. Dubrovsky and N. L. Abbott, *Science*, 1998, **279**, 2077–2080; (*b*) A. M. Lowe and N. L. Abbott, *Chem. Mater.*, 2012, **24**, 746–758; (*c*) I. H. Lin, D. S. Miller, P. J. Bertics, C. J. Murphy, J. J. de Pablo and N. L. Abbott, *Science*, 2011, **332**, 1297–1300; (*d*) P. M. Naveenkumar, S. Mann and K. P. Sharma, *Adv. Mater. Interfaces*, 2019, **6**, 1801593; (*e*) S. Aery, A. Parry, A. A. Calahorra, S. D. Evans, H. F. Gleeson, A. Dan and A. Sarkar, *J. Mater. Chem. C*, 2023, **11**, 5831–5845; (*f*) D. K. Nguyen and C. H. Jang, *Microchem. J.*, 2020, **156**, 104834–104840; (*g*) X. Yang, Y. Tian, F. Li, Q. Yu, S. F. Tan, Y. Chen and Z. Yang, *Langmuir*, 2019, **35**, 2490–2497; (*h*) X. Yang, X. Zhao, F. Liu, H. Li, C. X. Zhang and Z. Yang, *Soft Matter*, 2021, **17**, 4842–4847; (*i*) X. Yang and Z. Yang, *Langmuir*, 2022, **38**, 282–288.
9 (*a*) J. S. Park and N. L. Abbott, *Adv. Mater.*, 2008, **20**, 1185–1190; (*b*) K. Perera, T. M. Dassanayake, M. Jeewanthi, N. P. Haputhanthrige, S. D. Huang, E. Kooijman, E. Mann and A. Jákli, *Adv. Mater. Interfaces*, 2022, **9**, 2200891; (*c*) P. S. Noonan, P. Mohan, A. P. Goodwin and D. K. Schwartz, *Adv. Funct. Mater.*, 2014, **24**, 3206–3212; (*d*) X. Yang, H. Li, X. Zhao, W. Liao, C. X. Zhang and Z. Yang, *Chem. Commun.*, 2020, **56**, 5441–5444; (*e*) A. Borbora and U. Manna, *Langmuir*, 2022, **38**, 9221–9228; (*f*) X. Yang, X. Zhao, H. Zhao, F. Liu, S. Zhang, C. X. Zhang and Z. Yang, *Chem. – Asian J.*, 2022, **17**, e202101251; (*g*) U. Manna, Y. M. Zayas-Gonzalez, R. J. Carlton, F. Caruso, N. L. Abbott and D. M. Lynn, *Angew. Chem., Int. Ed.*, 2013, **52**, 14011–14015; (*h*) L. Yang, M. Khan and S. Y. Park, *RSC Adv.*, 2015, **5**, 97264–97271.
10 T. Gupta, A. K. Mondal, I. Pani, K. Chattopadhyay and S. K. Pal, *Soft Matter*, 2022, **18**, 5293–5301.
11 H. Sunshine and M. L. I. Arispe, *Curr. Opin. Lipidol.*, 2017, **28**, 408–413.
12 (*a*) X. Wang, P. Yang, F. Mondiot, Y. Li, D. S. Miller, Z. Chen and N. L. Abbott, *Chem. Commun.*, 2015, **51**, 16844–16847; (*b*) M. Sadati, A. I. Apik, J. C. Armas-Perez, J. Martinez-Gonzalez, J. P. Hernandez-Ortiz, N. L. Abbott and J. J. de Pablo, *Adv. Funct. Mater.*, 2015, **25**, 6050–6060; (*c*) J. M. Brake and N. L. Abbott, *Langmuir*, 2007, **23**, 8497–8507; (*d*) I. Pani, P. Madhu, N. Najiya, A. Aayush, S. Mukhopadhyay and S. K. Pal, *J. Phys. Chem. Lett.*, 2020, **11**, 9012–9018; (*e*) I. Verma, S. L. V. Selvakumar and S. K. Pal, *J. Phys. Chem. C*, 2020, **1**, 780–788; (*f*) T. Gupta, L. Arora, S. Mukhopadhyay and S. K. Pal, *J. Phys. Chem. Lett.*, 2024, **15**, 2117–2122.
13 E. Mulvihill, K. V. Pee, S. A. Mari, D. J. Müller and O. Yildiz, *Nano Lett.*, 2015, **15**, 6965–6973.
14 (*a*) D. Andrienko, M. Tasinkevych and S. Dietrich, *Europhys. Lett.*, 2005, **70**, 95–101; (*b*) G. M. Koenig Jr, I. H. Lin and N. L. Abbott, *Proc. Natl. Acad. Sci. U. S. A.*, 2010, **107**, 3998–4003.
15 T. Gupta, *Toxin-Induced Ordering Transitions of Liquid Crystals at Biomolecular Interfaces*, PhD thesis, IISER Mohali, 2024.

 